Coalescence of three silver nanoclusters: a molecular dynamics study

2001 J. Phys.: Condens. Matter 13 8061

(http://iopscience.iop.org/0953-8984/13/35/313)

INSTITUTE OF PHYSICS PUBLISHING JOURNAL OF PHYSICS: CONDENSED MATTER

J. Phys.: Condens. Matter **13** (2001) 8061–8069 PII: S0953-8984(01)26238-9

Coalescence of three silver nanoclusters: a molecular dynamics study

S J Zhao[1], **S Q Wang, Z Q Yang and H Q Ye**

Shenyang National Laboratory for Materials Science, Institute of Metal Research, Chinese Academy of Sciences, Shenyang 110016, People's Republic of China

E-mail: sjzhao@imr.ac.cn

Received 27 June 2001, in final form 23 July 2001
Published 16 August 2001
Online at stacks.iop.org/JPhysCM/13/8061

Abstract

Coalescence of three identical size nanoclusters, each containing 309 silver atoms interacting through an analytic embedded-atom method (EAM) type potential, is studied by molecular dynamics simulations at various temperatures. The rotation and spontaneous self-organization of all three clusters in the coalescence process are observed. The final low-energy configurations of the coalescing system at low temperatures ($T \leqslant 800$ K) are constituted of three particles separated by attached interfaces where edge dislocations are formed, whereas the coalescing at high temperatures ($T > 800$ K) gives rise to a single-like particle. The melting temperature of the coalescing system is well below that of the free single cluster with the same particle size.

1. Introduction

The coalescence process of nanoclusters continues to be a subject of active research of basic and technological interest, because it is of primary importance for understanding the structure of cluster-assembled materials. The macroscopic models currently available to treat this type of problem are based on the kinetic, thermodynamic and mechanical properties of solid that are typical of bulk crystals [1–3]. However, the situations may be very different in nanoparticles and a more atomistic approach is necessary. Computer simulation methods, in particular molecular dynamics (MD), are effective to investigate the details on an atomic level of the coalescence process involved in the building of these nanostructures. By employing the MD method, the coalescence processes of two copper [4] and two gold [5] clusters were investigated at 700 K and 800 K, respectively. Two distinct and generally sequential processes [6] which led to the coalescence of two nanoparticles, i.e. plastic deformation [4] and slow surface diffusion [5], were found. The simulation results [5, 6] also suggested that the classic theory [1] may not be entirely satisfactory for the coalescence of particles in the nanometre range.

[1] Formerly with the Laboratory of Atomic Imaging of Solids.

0953-8984/01/358061+09$30.00

In this work, we use MD technology to investigate the coalescence of three nanoclusters over a wide temperature range from 300 K to 1200 K. We focus here on the temperature influence on the atomic configuration of the coalescing system. For comparison, the melting processes of size-selected free single nanoparticles containing 258–3871 silver atoms are also simulated.

2. Simulation procedure

In all of our MD simulations, we used an analytic embedded-atom method (EAM) type potential [7], which was confirmed to be able to describe fractional density change on melting, heat of fusion, linear coefficients of thermal expansion and heat capacities above room temperature successfully [7]. In constant-temperature simulations by using the damped force method [8], the initial configurations of all free single clusters of $N = 258$–3871 atoms are arranged as truncated Marks decahedra (e.g. see the initial atomic structure of Ag_{309} in figure 1), and the relative crystallographic axes of the three 309-atom clusters before coalescing are symmetrically oriented (see the initial configuration of the coalescing system in figures 5(a) and (b)). All the simulations were performed by starting at 300 K, at which the system was run for 500 000 integration time steps ($\sim$100 ps), and then the temperature was elevated by rescaling the atomic velocities using the Verlet velocity algorithm. After the desired temperature was reached, the atomic configurations were recorded after equilibrating for 500 000 integration time steps. For each of the recorded configurations, another run of 100 000 time steps at the corresponding temperature was performed in order to determine the thermodynamic properties of the system.

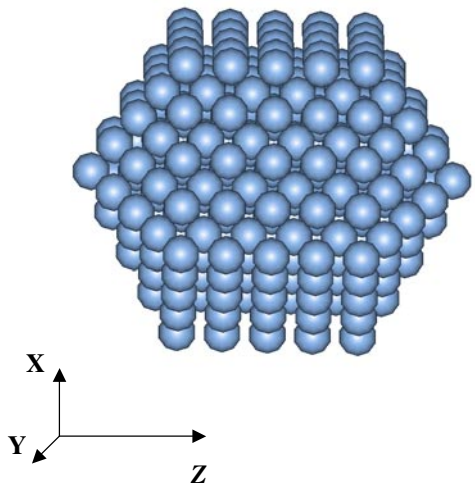

Figure 1. Snapshot of the initial structure (a truncated Marks decahedron) of the single cluster containing 309 silver atoms.

3. Results and analysis

We first consider the single clusters as a preliminary step toward the second stage of our study, namely coalescence. Figure 2 shows the caloric curves for the single particles with

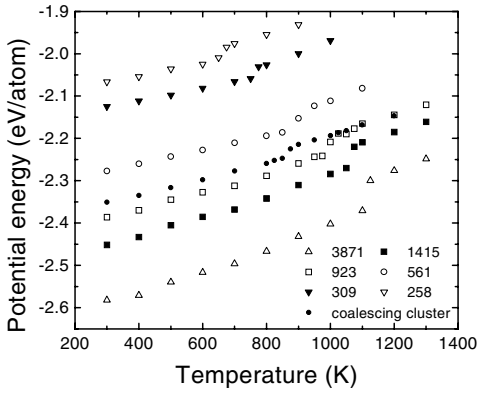

Figure 2. Temperature dependence of potential energy of the coalescing cluster (full circles) and free single clusters containing 258 to 3871 silver atoms.

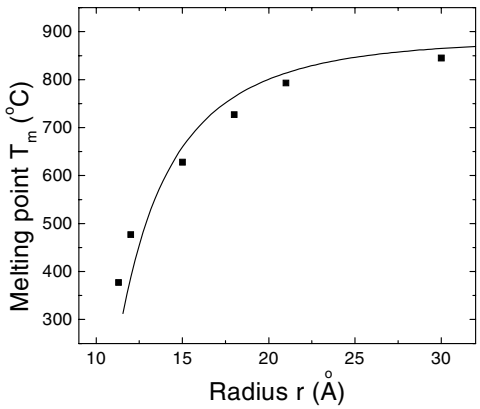

Figure 3. r dependence of the melting points of free single silver particles of $N = 258$–3871 atoms. The solid line is calculated in terms of equation (2).

size $N = 258$–3871 atoms, from which the melting temperatures of the particles (as shown in figure 3) are obtained. In order to state conveniently in the study for the coalescence, here we note that the melting temperatures of Ag_{309} and Ag_{923} are 750 K and 1000 K, respectively. In the following, we examine the size dependence of the melting point quantitatively by employing some phenomenological models.

According to the surface premelting models (SPMs) [9, 10], the melting temperature is taken to be the temperature of equilibrium between the solid sphere core and the concentric liquid shell of a given critical thickness t_0, which is an adjustable parameter [9, 11]. Neglecting the difference between the vapour pressure at the surface of the liquid layer at T_m and the pressure at flat liquid surface at T_0 (T_0 is the bulk melting temperature), one obtains [9, 11]

$$T_0 - T_m = \frac{2T_0}{\Delta\mu_0^{ls}}\left[\frac{\sigma_{sl}}{\rho_s(r - t_0)} + \frac{\sigma_{lv}}{r}\left(\frac{1}{\rho_s} - \frac{1}{\rho_l}\right)\right] \tag{1}$$

where r is the particle radius, $\Delta\mu_0^{ls}$ is the latent heat of fusion of bulk solid and t_0 is the critical thickness of the liquid layer at T_m. σ_{sl} is the interfacial surface tension between the solid and the liquid, while σ_{lv} is that between the liquid and its vapour. ρ_s and ρ_l are the densities of

the solid and liquid, respectively. Substituting $T_0 = 960.7\,^{\circ}\mathrm{C}$, $\Delta\mu_0^{ls} = 1.06 \times 10^9$ erg g^{-1}, $\rho_s = 10.49$ g cm^{-3}, $\rho_l = 9.35$ g cm^{-3} [12], $\sigma_{sl} = 184$ dyn cm^{-1} and $\sigma_{lv} = 910$ dyn cm^{-1} [13] into equation (1), we obtain

$$T_m = 960.7 - 2463\left(\frac{1}{0.603(r - t_0)} - \frac{1}{r}\right) \tag{2}$$

where T_m is in $^{\circ}$C, and r and t_0 are in Å.

By adjusting the value of t_0, we obtain a best fit to the simulated data in terms of equation (2) when $t_0 = 10.1$ Å (see figure 3), which indicates that the melting process of $Ag_{3871-258}$ can be described well by the SPM. The agreement also indicates that the potential [7] employed in the present work is reliable for prediction of thermodynamic properties of silver clusters.

The surface premelting in $Ag_{258-3871}$ can be identified by the calculations of the static structure factor S. In the calculations of S, the clusters were divided into a series of concentric shells. The static structure factor S, defined as

$$S = \frac{1}{N^2}\left|\sum_{j\in L}\exp(\mathrm{i}\vec{k}\vec{r}_j)\right|^2 \tag{3}$$

is calculated for each of the concentric shells. In the above expressions, L specifies the particular shell and N is the number of atoms in shell L. $\boldsymbol{k}$ is a prescribed wavevector and $\boldsymbol{r}_j$ is the position of atom j that belongs in shell L. At zero temperature S equals unity, while in the liquid it fluctuates close to zero [14, 15].

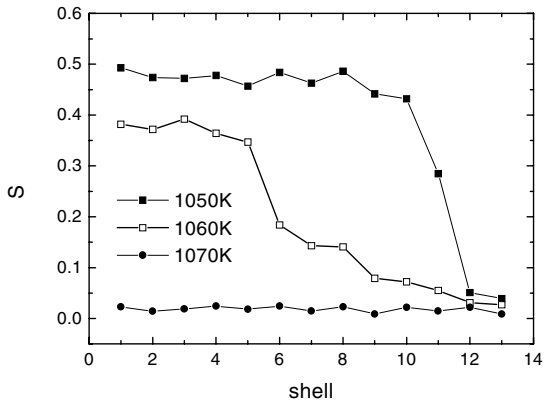

Figure 4. Shell-by-shell profiles of static structure factor S for Ag_{1415} at 1050 K, 1060 K and 1070 K.

Figure 4 shows the shell-by-shell profiles of S for Ag_{1415} at 1050 K, 1060 K and 1070 K (T_m). From the core region to the surface, the numbers of the shells are denoted by 1, 2, . . . , 13, respectively. It is clear from figure 4 that melting initiates at the surface. For the two outmost shells, the S values already reaches liquid-like values around a critical temperature $T_c \sim 1050$ K ($T_c < T_m$). When the temperature rises further, the decrease of S is clearly related to the progressive loss of crystalline order from the surface to the core region. When T_m ($\sim$1070 K) is reached, the liquid seed already present propagates to the whole particle.

There are several phenomenological models [9, 10, 16–18] proposed to account for the origin of the premelting and the melting point depression in nanoclusters. Almost all considered the cluster as consisting of 'bulk' and 'surface' atoms. The physical cause for the melting point depression lies in the fact that small clusters have a higher proportion of surface atoms. Surface

atoms have fewer nearest atoms and are thus more weakly bound and less constrained in their thermal motion [19, 20] than those in bulk. Upon a combined effect of thermal fluctuations and an intrinsic elastic instability in the system [21], the surface begins premelting at a critical temperature that is well below the bulk melting point. The premelting of the surface induces the melting of the whole cluster and thus leads to the melting point depression. Recently, Jiang *et al* [22–25] presented a model for size-dependent melting point depression based on the size-dependent amplitude of the atomic thermal vibrations of nanocrystals in terms of the Lindemann criterion. Since all the parameters in their model are only the well known bulk melting temperature and the bulk melting entropy, their model can predict the size-dependent and dimension-dependent melting temperature of any kind of nanocrystal.

Based on the results of the single clusters, the simulations for the coalescence of three 309-atom clusters are carried out over a wide temperature range from 300 K to 1200 K. In a similar way to the coalescence of two clusters [4, 5], the three clusters are drawn together quickly by the excess surface energy [4, 26] in the initial stage of coalescing. Subsequently, all three clusters rotate in space in order to find a low-energy configuration. The approach and rotation of the three clusters can be clearly seen from figure 5(b), which illustrates an example case at 300 K.

Visual inspection of the x–y plane projection of the atomic positions in figure 5(a) shows that the final low-energy configurations of the coalescing cluster at low temperatures ($T \leqslant 800$ K) are constituted of three particles separated by attached interfaces where edge dislocations are formed. Here the edge dislocations are defined as having a Burgers vector normal to the dislocation line, which are similar to those seen in low-angle tilt boundaries. As examples, two edge dislocations are denoted by the symbol '$\perp$' at 600 K in figure 5(a). The formation of edge dislocations at attachment interfaces could be explained as follows. When structurally similar surfaces of particles approach, there will be a driving force to form chemical bonds between atoms of opposing surfaces so as to achieve full coordination. However, typically, surfaces are not atomically flat. In addition, there is much higher vacancy concentration at attached interfaces, which leads to the bond contraction [27]. The curving surfaces and the bond contraction prevent atoms from achieving full coordination. Coherence will then be achieved by distortion in some areas of the interface. Edge dislocations will form in the regions of step sites when the axis of rotation (parallel to the z-axis in this work) is contained within the plane of the interface (perpendicular to the x–y plane in this work).

The substantial driving force for cluster rotation and reorganization to achieve full coherence is generally expected. However, at $T \leqslant 800$ K, some rotations and spontaneous self-organizations may be metastable and preserved by formation of a coincident site array.

At high temperatures ($T > 800$ K), thermal vibrations of atoms are enhanced significantly. Under these circumstances, the system can get over the potential barrier to achieve full coherence. As a result, the coalescing at $T > 800$ K gives rise to a single-like particle (see the atomic configurations at 825 K and 850 K in figure 5(a)), which is formed on the basis of proper rotation and reorganization of the three constituent clusters. The perfect bonding between the clusters reduces the overall energy by removing the surface energy associated with unsatisfied bonds.

All these are different from the coalescence of two nanoparticles, in which two particles rotated until a low-energy boundary was formed [4].

The slow surface diffusion, which was observed in the simulations of coalescence of two gold nanoclusters by Lewis, Jensen *et al* [5, 6], can also be seen from figure 5(a). Even after 50 000 MD steps equilibrating, very few atoms have managed to diffuse a significant distance away from the contact region of the three clusters at temperature range between 300 K and 850 K.

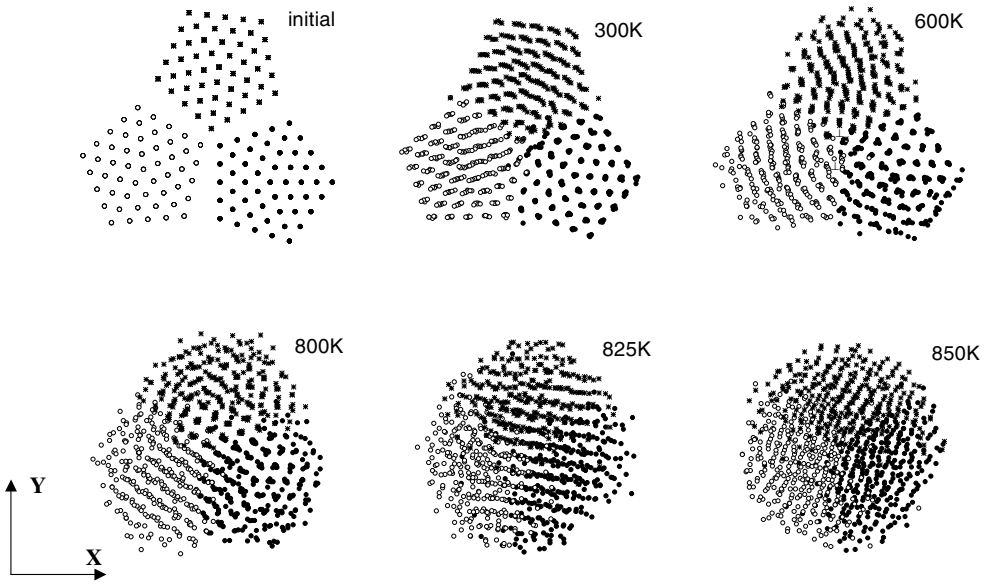

(a)

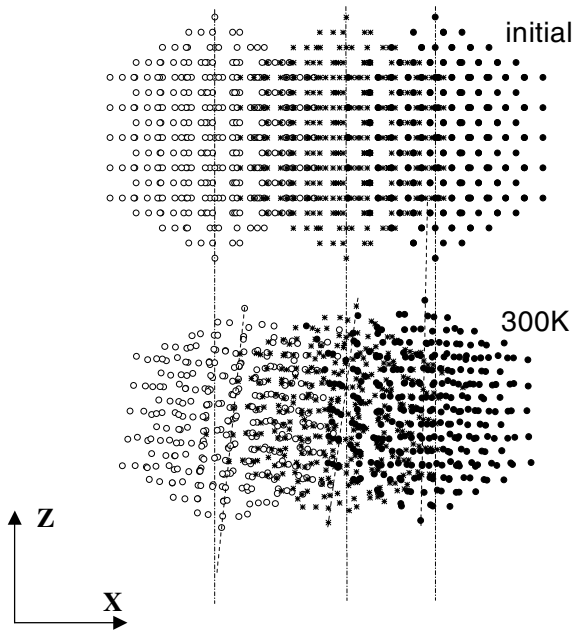

(b)

Figure 5. (a) The x–y plane projection of the initial (top left) and the final atomic configurations of the coalescing cluster at temperature range between 300 K and 850 K. As examples, two edge dislocations are denoted by the symbol '$\perp$' at 600 K. (b) The x–z plane projection of the initial (top) and the final (bottom) atomic configurations of the coalescing cluster at 300 K. The centroidal principal axes of the three constituent clusters in the initial and the final atomic configurations are denoted by dash–dot and dashed lines, respectively, which illustrate approach and reorientation of the three constituent clusters during coalescing.

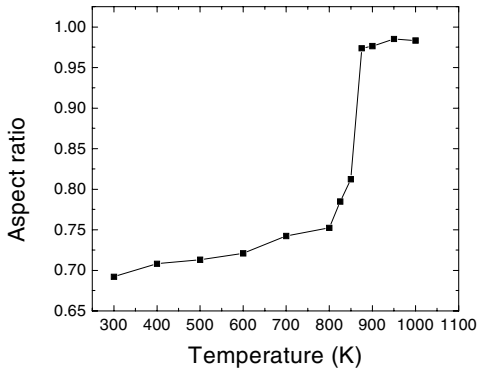

Figure 6. Temperature dependence of the aspect ratio of the coalescing cluster after 500 000 MD steps equilibrating.

The orderly atomic configuration and slow surface diffusion both indicate that the coalescing cluster is completely solid when $T \leqslant 850$ K, though at $T \geqslant 750$ K the three constituent clusters have already molten when they are single and free.

What happens now when the coalescing cluster melts? When clusters melt they are expected to adopt the roughly spherical geometry of a liquid droplet [5, 6, 28]. Here, we discuss the melting behaviour of the coalescing cluster by investigating its sphericization process. The three principal moments of inertia I, defined as

$$I_\alpha = \sum(\beta^2 + \gamma^2)m$$

in the centre of mass frame, are calculated during the simulations. In the above expression, α, β and γ are the three components of the coordinates, and m is the atomic mass of silver. For a system that can rotate in space, the ratio of the smallest to the largest of the three principal moments of inertia is an effective measure of the 'aspect ratio' for the sphericization [5]. Figure 6 shows the aspect ratio of the final atomic configuration after 50 000 MD steps equilibrating at various temperatures. The aspect ratio increases very slowly with temperature up to 850 K, then rises sharply when temperature is raised further. The value of the aspect ratio reaches 0.9737 when temperature is raised up to 875 K, which is typical of a spherical liquid droplet. It should be noted that, in fact, the value of the aspect ratio at 875 K has increased to 0.9432 in the first MD run of about 9000 integration time steps. This is to say, the sphericization of the coalescing cluster at 875 K is very rapid, though it is a much slower process at lower temperatures and the time scale for such a process is a few hundred nanoseconds or more [5]. The molten phase of the coalescing cluster at 875 K can be identified by the calculations of the potential energy, which would jump to a higher value of liquid at the melting point [14, 15].

Figure 2 also shows the caloric curve for the coalescing cluster, in which the melting of the coalescing cluster can be clearly identified by an upward jump in energy at 875 K. In addition, typical signatures of the melting obtained from the caloric curves between the coalescing cluster and the single cluster with a comparable particle size, namely Ag_{923}, are (i) the solid branch of the coalescing cluster is higher than that of Ag_{923}, while the liquid branches of them are nearly overlapped, and (ii) the melting temperature (875 K) of the coalescing cluster is 125 K lower than that (1000 K) of Ag_{923}. We ascribe these signatures to the following facts: (i) compared to Ag_{923} the energy of the coalescing cluster is enhanced due to the existing cluster–cluster bonding region at temperatures below 875 K, while both differences in the energy and morphology disappear when they are in liquid, and (ii) besides the surface, the

cluster–cluster bonding regions act as the heterogeneous nucleation sites in the melting of the coalescing cluster, which facilitates the melting and depresses the melting point.

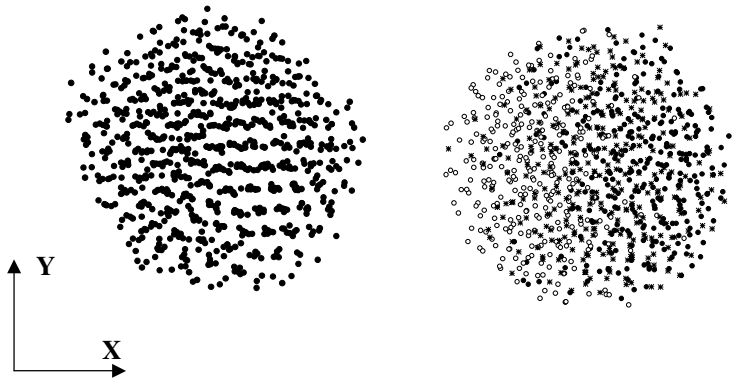

Figure 7. The x–y plane projection of the atomic configurations of Ag_{923} (left) and the coalescing cluster (right) at 875 K.

Figure 7 shows the x–y plane projections of the atomic positions of Ag_{923} (left) and the coalescing cluster (right) at 875 K. It is clear from this figure that at 875 K the atomic structure of Ag_{923} is still crystalline, while the coalescing cluster has already been definitely liquid.

4. Summary

The temperature dependence of the coalescence of three silver nanoclusters has been investigated in this work. At low temperatures ($T \leqslant 800$ K), the coalescing system is constituted of three particles separated by attached interfaces where edge dislocations are formed. At high temperatures ($T > 800$ K), the final low-energy configuration of the coalescing system is a single-like particle. For comparison, the melting of size-selected free single nanoparticles containing 258–3871 atoms is also simulated and the size-dependent melting temperature depression of the particles agrees well with the prediction of the surface premelting models. The simulation results indicate that the melting temperature of the coalescing system is well below that of the free single cluster with the same particle size.

Acknowledgments

We acknowledge financial support of this work by the Special Funds for the Major State Basic Research Projects (No G2000067104) and the National Natural Science Foundation (No 59831020) of China.

References

[1] Nichols F A 1966 *J. Appl. Phys.* **37** 2805
[2] Kellet B J and Lange F F 1989 *J. Am. Ceram. Soc.* **72** 725
[3] Soppe W J, Janssen G L, Bonekamp B C, Correia L A and Veringa H J 1994 *J. Mater. Sci.* **29** 752
[4] Zhu H and Averback R S 1996 *Phil. Mag. Lett.* **73** 27
[5] Lewis L, Jensen P and Barrat J-L 1997 *Phys. Rev.* B **56** 2248
[6] Jensen P 1999 *Rev. Mod. Phys.* 71 1695
[7] Mei J, Davenport J W and Fernando G W 1991 *Phys. Rev.* B **43** 4653

[8] Evans D J 1983 *J. Chem. Phys.* **78** 3297
[9] Wronski C R M 1967 *Br. J. Appl. Phys.* **18** 1731
[10] Kofman R, Cheyssac P, Aouaj A, Lereah Y, Deutscher G, David T B, Penisson J M and Bourret A 1994 *Surf. Sci.* **303** 231
[11] Lai S L, Guo J Y, Petrova V, Ramanath G and Allen L H 1996 *Phys. Rev. Lett.* **77** 99
[12] Shi C X 1995 *Cyclopaedia of Materials Science and Technology* 1st edn (Beijing: Chinese Cyclopaedia) p 1202
[13] Pluis B, Frenkel D and van der Veen J F 1990 *Surf. Sci.* **239** 282
[14] Zhao S J, Wang S Q, Zhang T G and Ye H Q 2000 *J. Phys.: Condens. Matter* **12** L549
[15] Zhao S J, Cheng D Y, Wang S Q and Ye H Q 2001 *J. Phys. Soc. Japan* **70** 733
[16] Pawlow P 1909 *Z. Phys. Chem.* **65** 1
[17] Reiss H and Wilson I B 1948 *J. Colloid Sci.* **3** 551
[18] Buffat Ph and Borel J-P 1976 *Phys. Rev.* A **13** 2287
[19] Couchman R R 1979 *Phil. Mag.* A **40** 637
[20] Berry R S 1990 *Sci. Am.* **263** 50
[21] Jin Z H, Sheng H W and Lu K 1999 *Phys. Rev.* B **60** 141
[22] Jiang Q, Aya N and Shi F G 1997 *Appl. Phys.* A **64** 627
[23] Jiang Q, Tong H Y, Hsu D T, Okuyama K and Shi F G 1998 *Thin Solid Films* **312** 357
[24] Jiang Q, Shi H X and Zhao M 1999 *J. Chem. Phys.* **111** 2176
[25] Z Zhang, J C Li and Q Jiang 2000 *J. Phys. D: Appl. Phys.* **33** 2653
[26] Johnson K L, Kendall K and Roberts A D 1971 *Proc. R. Soc.* A **324** 301
[27] Yu X F, Liu X, Zhang K and Hu Z Q 1999 *J. Phys.: Condens. Matter* **11** 937
[28] Shvartsburg A A and Jarrold M F 2000 *Phys. Rev. Lett.* **85** 2530